

---

# Exploring 3D Activity Reasoning and Planning: From Implicit Human Intentions to Route-Aware Planning

---

Xueying Jiang<sup>1</sup> Wenhao Li<sup>1</sup> Xiaoqin Zhang<sup>2</sup> Ling Shao<sup>3</sup> Shijian Lu<sup>1\*</sup>

<sup>1</sup>College of Computing and Data Science, Nanyang Technological University, Singapore

<sup>2</sup>College of Computer Science and Technology, Zhejiang University of Technology, China

<sup>3</sup>UCAS-Terminus AI Lab, University of Chinese Academy of Sciences, China

## Abstract

3D activity reasoning and planning has attracted increasing attention in human-robot interaction and embodied AI thanks to the recent advance in multimodal learning. However, most existing studies are facing two common challenges: 1) heavy reliance on explicit instructions with little reasoning on implicit user intention; 2) negligence of inter-step route planning on robot moves. We address the above challenges by proposing 3D activity reasoning and planning, a novel 3D task that reasons the intended activities from implicit instructions and decomposes them into steps with inter-step routes and planning under the guidance of fine-grained 3D object shapes and locations from scene segmentation. We tackle the new 3D task from two perspectives. First, we construct ReasonPlan3D, a large-scale benchmark that covers diverse 3D scenes with rich implicit instructions and detailed annotations for multi-step task planning, inter-step route planning, and fine-grained segmentation. Second, we design a novel framework that introduces progressive plan generation with contextual consistency across multiple steps, as well as a scene graph that is updated dynamically for capturing critical objects and their spatial relations. Extensive experiments demonstrate the effectiveness of our benchmark and framework in reasoning activities from implicit human instructions, producing accurate stepwise task plans and seamlessly integrating route planning for multi-step moves. The dataset and code will be released.

## 1 Introduction

With the rapid development of multimodal learning, 3D activity reasoning and planning has become one essential component in various robot tasks that involve frequent interactions with humans and 3D world. Traditional robot task planning relies heavily on explicit instructions. However, it is critical to empower robots to reason the intended activity from implicit human instructions since human instructions in natural language are often ambiguous and imprecise. In addition, the ability of generating a detailed task plan for the reasoned activity is critical as well for navigating in 3D scenes, interacting with relevant scene objects, and accomplishing complex real-world tasks. At present, reasoning implicit human instructions, and further planning a reasonable sequence of executable steps with inter-step routes remains a grand challenge in human-robot interaction and embodied AI.

Several prior studies [52, 44, 46, 7, 18] have investigated 3D activity reasoning and planning, but most struggle in activity reasoning from implicit instructions and inter-step route planning. For example, ALFRED [44] achieves task planning based on explicit instructions, but it cannot accurately reason specific activities from vague or implicit human instructions. [52] studies how to decompose human

---

\*Corresponding author.

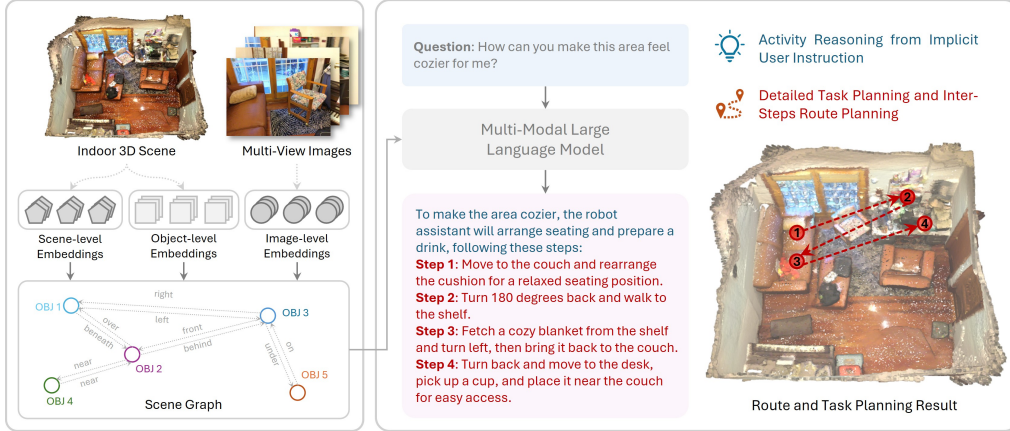


Figure 1: The proposed 3D Activity Reasoning and Planning enables reasoning activities underneath user’s implicit instructions. It can generate detailed executable steps for the reasoned activities within 3D scenes, as well as consistent inter-step route planning with object shapes and object locations derived from fine-grained 3D segmentation.

instructions into separate action steps, but they focus on task decomposition only without considering much about inter-step route planning. As of today, most existing approaches are facing various challenges while addressing activity reasoning, task planning, and route planning simultaneously, struggling with comprehending user’s implicit instructions and generating route plans.

We propose 3D activity reasoning and planning, a novel 3D task that reasons the underlying intention and activities from implicit human instructions, decomposes the reasoned activities into multiple executable step-by-step plans, and performs inter-step route planning with 3D scene understanding. We tackle the new 3D task from two perspectives. First, we construct ReasonPlan3D, a large-scale and comprehensive benchmark that comprises diverse 3D scenes, various implicit human instructions and corresponding activities, detailed step-by-step plans, and annotations of the inter-step route planning. The benchmark comprises segmentation annotations of objects in scenes which benefit 3D scene understanding and concurrently provide fine-grained guidance for generating accurate route planning between steps. ReasonPlan3D features superb diversity in actions, objects, and movement types, supporting complex reasoning and planning across a broad spectrum of 3D activity scenarios.

In addition, we design SHARP, a novel 3D activity reasoning and planning framework that enables Scene-graph-based Activity Reasoning and Planning from implicit user instructions and generates executable plans with detailed routes between steps. The framework comes with a novel progressive plan generation strategy that produces the step-by-step planning by referring to historical steps, enabling contextual consistency throughout all planned steps for the reasoned activity. We construct a scene graph for each scene to model the relation among various objects in scenes, and design dynamic graph modulation (DGM) to update the scene graph for adaptive identification of target objects and their spatial relations with respect to the reasoned activity. The DGM guides the model to focus on the objects that are critical to the reasoned activity, thereby providing highlighted information for the subsequent route planning under the assistance of spatial relations among relevant objects. As illustrated in Figure 1, our framework can effectively interpret the intention underneath the implicit human instruction, precisely reasoning out the desired activity, and producing detailed and coherent execution steps with inter-step route planning.

The major contributions of this work can be summarized in three aspects. First, we propose a new 3D activity reasoning and planning task based on implicit human instructions, together with a large-scale and high-quality benchmark. The benchmark covers various implicit human instructions and annotations of detailed planning for the intended activity, including executable steps and inter-step routes under the guidance of 3D scene segmentation. The benchmark provides a valuable platform for designs and evaluations in the area of 3D activity reasoning and planning. Second, we design a novel framework that incorporates progressive plan generation for context-aware planning, as well as dynamic graph modulation for capturing critical objects and their relations, achieving effective 3D activity reasoning and planning. Third, extensive experiments demonstrate the superiority and great value of our proposed approach and benchmark in 3D Activity Reasoning and Planning.

## 2 Related Work

### 2.1 Embodied Large Language Model Planning

In the area of embodied task planning, there are various works [30, 52, 54, 55, 5, 59, 27, 40, 46, 26] that leverage large language models to generate executable action plans. Specifically, LLM-based approaches generate action plans either through direct environmental input [27, 57, 40, 46, 30, 52, 5] or via prompt engineering [26]. Recent studies enhance planning by evaluating action affordances [4, 16], employing code-driven policies [45], and leveraging commonsense knowledge from world models [12, 15, 36]. For example, AdaPlanner [47] adaptively refines its self-generated plans using environmental feedback. Grounded 3D-LLM [7] performs instance segmentation of relevant objects yet lacks route planning capabilities. SG3D [57] relies on explicit human instructions to perform sequential object grounding. Unlike existing approaches [52, 7, 57] that focus on isolated action steps and rely on explicit user instructions to specify the target activity, our work introduces inter-step route planning and reasons human intentions from implicit user inputs, enabling robots to execute tasks within complex 3D environments.

### 2.2 Language-Instructed 3D Scene Understanding

Recent studies in 3D scene understanding [17, 23, 28, 35, 43] increasingly leverage natural language to enrich contextual knowledge and capture user intentions for human-model interactions. Existing research primarily focuses on tasks such as visual grounding [25, 58, 14, 53, 5, 18, 29], 3D question answering [2, 34, 38, 13, 18], 3D referring [17, 24, 39, 51], and 3D dense captioning [8, 6, 18]. With the advance in large language models (LLMs) [48], several recent studies [50, 11, 22, 21, 18, 5, 10] explore 3D LLMs, aiming to bridge the gap between text and 3D scenes. For example, Chat-Scene [20] employs object identifiers for accurate 3D scene referencing and represents the 3D scene with instance-level features from pre-trained 2D and 3D models. Grounded 3D-LLM [7] uses referent tokens and contrastive language-scene pre-training to achieve scene-text alignment. Recently, 3DGraphLLM [56] constructs a 3D scene graph to explicitly capture the semantic relations among objects. In contrast, our work introduces a novel 3D Activity Reasoning and Planning task that simultaneously reasons implicit human intentions and performs task planning with integrated inter-step route planning, addressing a critical gap in existing approaches.

## 3 ReasonPlan3D Benchmark

Most existing benchmarks [52, 44, 7, 57, 18, 41, 31] for task planning in 3D scenes are not well-suited for exploring the task of 3D Activity Reasoning and Planning. Specifically, existing 3D task planning benchmarks share two major constraints as illustrated in Table 1. First, existing 3D task planning benchmarks are designed for models to follow explicit human instructions regarding the desired activity. They do not provide data for training models for reasoning about humans’ implicit intentions about specific activities, thereby limiting the model’s capability in discovering the underlying human intentions. Second, most existing 3D task planning benchmarks [31, 52, 7] focus on isolated action steps while planning a task, neglecting inter-step route planning and hindering the robot assistant from seamlessly interacting with the surrounding 3D environment. We address the two limitations by proposing a data generation pipeline together with a comprehensive benchmark ReasonPlan3D, with more details to be elaborated in the following subsections.

### 3.1 ReasonPlan3D Content

In the proposed ReasonPlan3D, each scene represented by point clouds  $P$  and multi-view images  $I_{mv}$  is paired with multiple triplets  $\{X_{inst}, Y_{plan}, M_{3D}\}$ . Here,  $X_{inst}$  is an implicit human instruction requiring the model to reason the user’s underlying intended activities;  $Y_{plan}$  is a step-by-step plan with inter-step route planning; and  $M_{3D}$  denotes instance segmentation masks for the objects involved in  $Y_{plan}$ , providing fine-grained guidance with object shapes and locations for route planning. Specifically,  $x_{inst}$  is formulated to avoid explicit statements of the desired activity. For example, instead of saying “Please help me make a cup of coffee,” the instruction would be “I want to feel refreshed in the morning in this space. How could you help me?” Consequently,  $Y_{plan}$  first reasons the intended activity (e.g., preparing coffee) from the implicit instruction, then plans detailed steps

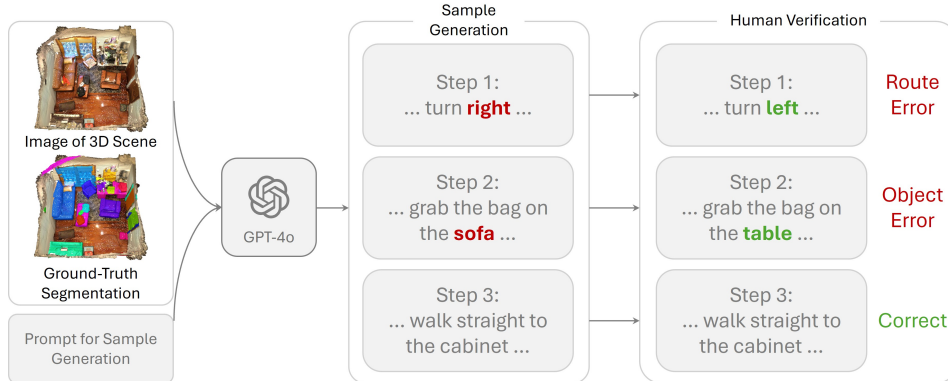


Figure 2: The pipeline of ReasonPlan3D generation. Given a 3D scene image, its corresponding ground-truth segmentation, and the designed prompt, GPT-4o generates a sample including implicit human instructions and step-by-step task planning together with answers to inter-step route planning. The generated sample is then verified by humans for correcting errors in routes, objects, etc.

Table 1: 3D activity reasoning and planning benchmarks. The proposed ReasonPlan3D excels in its large-scale and high-quality data samples, enabling a wide spectrum of evaluations including task planning, activity reasoning from implicit instructions, inter-step route planning, and segmentation.  $IP\ Pair$  denotes the Instruction-Plan pair  $\{X_{inst}, Y_{plan}\}$ .

| Benchmark           | Source     | Scale   |           | Capabilities of Each IP Pair |                    |                |                 |
|---------------------|------------|---------|-----------|------------------------------|--------------------|----------------|-----------------|
|                     |            | # Scene | # IP Pair | Task Planning                | Activity Reasoning | Route Planning | 3D Segmentation |
| ALFRED [44]         | Simulation | 120     | 25K       | ✓                            | ×                  | ✓              | ×               |
| BEHAVIOR-1K [31]    | Simulation | 50      | 1,000     | ✓                            | ×                  | ×              | ✓               |
| TaPA [52]           | Simulation | 80      | 15K       | ✓                            | ×                  | ×              | ×               |
| SG3D [57]           | Real World | 4,895   | 22K       | ✓                            | ×                  | ×              | ×               |
| SG3D-Nav [57]       | Simulation | 181     | 2,868     | ×                            | ×                  | ✓              | ×               |
| Grounded 3D-LLM [7] | Real World | -       | 4.4K      | ✓                            | ×                  | ×              | ✓               |
| ReasonPlan3D (Ours) | Real World | 1,513   | 27K       | ✓                            | ✓                  | ✓              | ✓               |

and corresponding inter-step route planning in the 3D scene. A sample  $Y_{plan}$  in response to the above instruction could be: “To help you feel refreshed, the robot assistant will prepare a cup of coffee for you, with the following steps: Step 1: Walk straight ahead to the kitchen counter. Step 2: Turn 90 degrees left and pick up the water kettle. Fill it with water from the sink. Step 3: Turn 90 degrees right and position the kettle on the stove. Step 4: Move to the coffee machine and add coffee grounds. Step 5: Once the water is heated, pour it into the coffee machine. Step 6: After brewing, grab the mug filled with coffee and deliver it to the table.”

### 3.2 ReasonPlan3D Generation Pipeline

We propose a novel benchmark generation pipeline leveraging GPT-4o to collect data samples. As illustrated in Figure 2, we provide GPT-4o with both the scene image and its ground-truth instance segmentation, enabling it to better identify and understand individual objects. The input prompt guides GPT-4o to generate implicit human instructions as well as step-by-step task planning with answers to inter-step route planning. For each generated sample, we conduct human verification and correct errors if any to ensure its quality. We particularly check for errors in route planning and objects, as GPT-4o frequently confuses directions, spatial relations, and objects in 3D scenes. We also check and rectify regarding the feasibility of the generated plans. All rectifications are made strictly based on factual inaccuracies to avoid introducing human preference or subjective bias. Overall, GPT-4o generates high-quality and contextually relevant data samples with quite limited manual correction, making it a reliable foundation in our benchmark generation.

### 3.3 ReasonPlan3D Statistics

The proposed ReasonPlan3D benchmark comprises a total of 1,513 scenes and 27,608 data samples, including point clouds and multi-view images sourced from ScanNet200 [42]. Following the split in [9, 42], we divide ReasonPlan3D into training and validation sets with 1201 and 312 scenes,

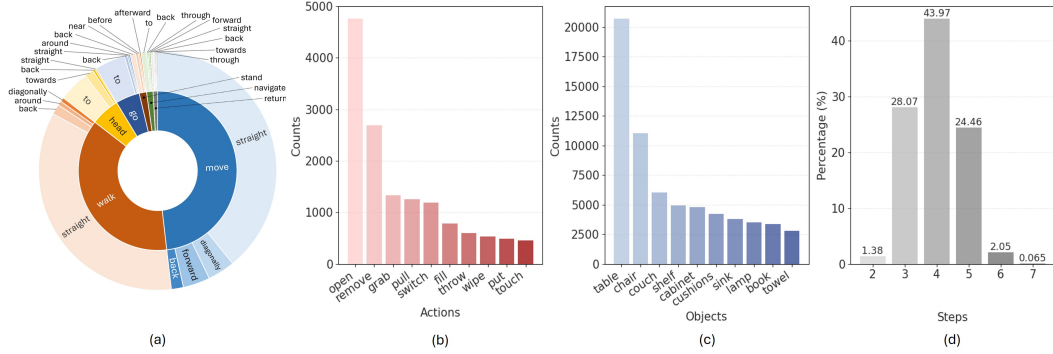


Figure 3: Benchmark statistics. The pie chart in (a) shows the most frequently occurring verbs in inter-step route planning, along with their associated adverbs representing movements. The bar charts in (b) and (c) present actions and their associated objects in the step-by-step plans, and that in (d) show the distribution of answers across different step counts.

respectively. On average, each scene in the benchmark includes 18.25 instructions, and each textual answer  $Y_{plan}$  comprises 3.98 steps and 76.67 words. The benchmark includes 200 distinct object categories for instance segmentation. As illustrated in Figure 3 (a), ReasonPlan3D encompasses a diverse range of movement categories along with their corresponding adverbs in inter-step route planning. Moreover, Figures 3 (b) and (c) showcase various actions, such as “open”, “remove”, and “grab”, along with the associated objects in these actions, demonstrating the richness of interactions with 3D Scenes. Additionally, as Figure 3 (d) shows, the distribution of textual answer lengths indicates the complexity of activity planning in our benchmark, with 28.07%, 43.97%, and 24.46% of answers comprising 3, 4, and 5 steps, respectively.

## 4 Method

### 4.1 Task Definition

3D Activity Reasoning and Planning task takes point clouds  $P$ , multi-view images  $I_{mv}$ , and user implicit instruction  $X_{inst}$  as input, aiming to reason the implicit intention for which activity  $A$  the user intend to perform and produce step-by-step plan  $\hat{Y}_{plan}$  with inter-step route planning, taking the fine-grained shape and location guidance from segmentation masks  $\hat{M}_{ins}$  of relevant objects in  $\hat{Y}_{plan}$ .

### 4.2 Overall Framework

Figure 4 illustrates the proposed framework of **SHARP**, which enables **Scene-graphH**-based **Activity Reasoning and Planning** based on implicit user instructions and generates detailed plans with inter-step routes. The input point clouds  $P$  are fed into the Point Cloud Encoder and the 3D Segmentor to produce scene-level embeddings  $F_{scene}$  and 3D segmentation masks  $M_{3D}$ , respectively. Besides, the 2D Encoder extracts features  $F_{mv}$  from multi-view images  $I_{mv}$ . Then  $M_{3D}$  and  $F_{mv}$  are passed to the Scene Graph Generator to obtain the scene graph  $G$ , which is then processed by the Graph Encoder to obtain object-level embeddings  $F_{obj}$ . Next,  $F_{scene}$  and  $F_{obj}$ , as well as implicit human instructions  $X_{inst}$  are taken as input into the Multi-Modal Large Language Model (MLLM) fine-tuned via LoRA [19]. At step  $s$ , the MLLM generates a one-step plan  $\hat{Y}_{plan}^s$  and obtains the graph modulation weights  $w_l$ . The plans of historical steps  $\{\hat{Y}_{plan}^1, \dots, \hat{Y}_{plan}^s\}$  are then fed into the MLLM to guide the next step. The graph modulation weights  $w_l$  adjust the scene graph  $G$  to emphasize objects and their spatial relations relevant to the reasoned activity, benefiting route planning.

### 4.3 Progressive Plan Generation

Contextual information is essential for ensuring consistency across steps in our activity planning task. To this end, we propose a progressive plan generation approach that explicitly enforces constraints among different steps by leveraging previously generated steps within a single plan. As illustrated in

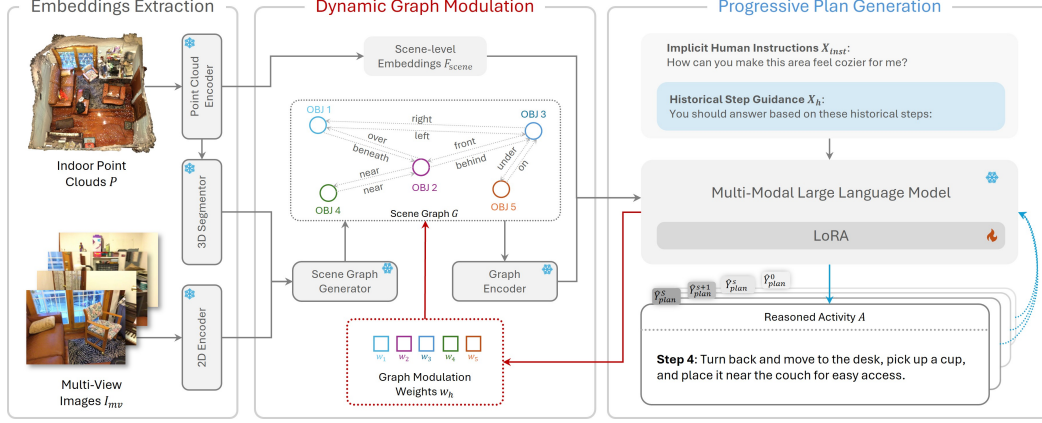


Figure 4: Overall architecture of the proposed SHARP method. Given the point clouds  $P$  of a 3D scene, the Point Cloud Encoder generates scene-level embeddings  $F_{scene}$ , while the 3D segmentor predicts 3D object masks. Besides, the 2D Encoder extracts multi-view image features  $F_{mv}$ , which are combined with 3D object masks as input to the Scene Graph Generator to obtain scene graph  $G$ . The generated scene graph  $G$  is then fed into the Graph Encoder, together with the scene-level embedding  $F_{scene}$  as the inputs of the MLLM. For step  $s$ , the one-step plan  $\hat{Y}_{plan}^s$  is generated by referring to previous steps, and the scene graph  $G$  is updated by graph modulation weights  $w_l$  that emphasize objects and their spatial relations that are critical to the reasoned activity. The snow icon indicates frozen modules, while the fire icon indicates trainable modules.

Algorithm 1, for each activity plan, we provide the human’s implicit instruction  $X_{inst}$  as input to the LLM while generating the first step. For subsequent steps, we prompt the LLM with an input historical step guidance template  $X_h$ , which incorporates previously generated plans and explicitly instructs the LLM to follow them. Specifically:

Q: {Human implicit instruction}. You should answer based on these historical steps: {plans of historical steps}.

Here, {human implicit instruction} is replaced with  $X_{inst}$  and {plans of historical steps} is substituted for  $\{\hat{Y}_{plan}^1, \dots, \hat{Y}_{plan}^{s-1}\}$ . Besides, for step  $s$ , only the ground truth of this step’s plan  $Y_{plan}^s$  is provided to supervise the learning of predicting  $\hat{Y}_{plan}^s$  consistently with historical steps.

To prevent the LLM from generating an excessive number of steps, we introduce a stop token [END] appended to the generated plan for the final step. Once the LLM outputs [END], it ceases plan generation, thus keeping the number of steps within a reasonable range. The token [END] is incorporated into the LLM’s token vocabulary to enable this functionality.

#### 4.4 Dynamic Graph Modulation

We propose a dynamic graph modulation mechanism that adaptively adjusts the importance of nodes and edges in the generated scene graph, thereby enhancing the awareness of relevant objects in the generated action plan. Specifically, the generated scene graph  $G$  consists of nodes

#### Algorithm 1 Pipeline of the Proposed SHARP

- 1: Initialization:
- 2: Scene graph  $G = \{N, E\}$ , scene-level embedding  $F_{scene}$ , and object-level embedding  $F_{obj}$  encoded from  $G$
- 3: **for** step  $s = 1$  **to**  $s = S$  **do**
- 4:   **if**  $s = 1$  **then**
- 5:      $X_{inst}$ ,  $F_{scene}$ , and  $F_{obj}$  input into LLM
- 6:   **end if**
- 7:   **if**  $s \neq 1$  **then**
- 8:      $X_{inst} \cup X_h \cup \{\hat{Y}_{plan}^1, \dots, \hat{Y}_{plan}^{s-1}\}$ ,  $F_{scene}$ , and  $F_{obj}$  input into the LLM
- 9:   **end if**
- 10:   **if**  $s = 1$  **then**
- 11:     Reasoning Activity  $A$
- 12:   **end if**
- 13:    $\hat{Y}_{plan}^s$  generated by the LLM
- 14:   **if** [END] in  $\hat{Y}_{plan}^s$  **then**
- 15:     **break**
- 16:   **end if**
- 17:   **if**  $i$ -th object in  $\hat{Y}_{plan}^s$  **then**
- 18:      $N_i * w_l$
- 19:     **for** neighbor  $j = 1$  **to**  $j = K$  **do**
- 20:        $N_{ij} * w_l$
- 21:        $E_{ij} * w_l$
- 22:     **end for**
- 23:   **end if**
- 24: **end for**

Table 2: Benchmarking on the ReasonPlan3D validation set for the 3D reasoning and planning task with evaluation metrics BLEU, CIDEr, METEOR, and ROUGE. Best in **bold**, second underlined.

| Method          | Venue      | BLEU-1       | BLEU-2       | BLEU-3       | BLEU-4       | CIDEr        | METEOR       | ROUGE        |
|-----------------|------------|--------------|--------------|--------------|--------------|--------------|--------------|--------------|
| 3D-LLM [18]     | NeurIPS 23 | 34.47        | 25.73        | 21.59        | 16.52        | 10.02        | 18.61        | 40.29        |
| LL3DA [5]       | CVPR 24    | 38.21        | 28.92        | 22.74        | 19.86        | 10.93        | 21.55        | 40.72        |
| Chat-Scene [20] | NeurIPS 24 | 39.47        | 31.04        | <u>25.80</u> | <u>21.15</u> | 11.67        | 21.94        | 42.28        |
| 3DGraphLLM [56] | arXiv 24   | <u>40.29</u> | <u>31.37</u> | 25.37        | 20.98        | <u>11.82</u> | <u>22.51</u> | <u>43.60</u> |
| SHARP (Ours)    | -          | <b>52.22</b> | <b>39.30</b> | <b>30.58</b> | <b>24.59</b> | <b>25.51</b> | <b>27.51</b> | <b>43.76</b> |

$N$  (representing objects) and edges  $E$  (representing spatial relations between two objects). When the generated one-step plan  $\hat{Y}_{plan}^s$  includes the  $i$ -th object  $N_i$ , we emphasize  $N_i$ , its  $K$  neighbors and their spatial relations by applying a larger weight  $w_l$  to the embeddings, as formulated below:

$$\{N_i, N_{ij}, E_{ij}\} * w_l, j \in \{1, \dots, K\} \quad (1)$$

where node  $N_{ij}$  denotes the  $j$ -th neighbor of  $N_i$ , and edge  $E_{ij}$  represents the spatial relation between  $N_{ij}$  and  $N_i$ . Here, the  $K$  neighbors of node  $N_i$  are selected using the K-Nearest Neighbors (KNN) algorithm. This mechanism can effectively coordinate with the proposed Progressive Plan Generation approach in the iterative process, as illustrated in Algorithm 1.

By focusing on the included objects, their most relevant neighbors, and corresponding spatial relations, this dynamic graph modulation mechanism improves the awareness of critical objects and their spatial relations which is beneficial for route planning within our task.

#### 4.5 Training Objective

For the textual responses generated by the LLM, we optimize the activity reasoning, step-by-step planning, and inter-step route planning using the following loss:

$$L_{plan} = CE(Y_{plan}, \hat{Y}_{plan}), \quad (2)$$

where  $CE(\cdot)$  denotes the cross-entropy loss. We train the proposed model end-to-end using  $L_{plan}$ .

## 5 Experiment

### 5.1 Experimental Settings

**Evaluation Metrics.** We adopt BLEU [37], ROUGE [32], METEOR [3], and CIDEr [49] to evaluate the quality of generated plans for the reasoned activities. In addition, we adopt BLEU-4, CIDEr, and METEOR to measure the performance of activity reasoning. Since our task centers on human-robot interaction and textual response generation, particularly for activity reasoning and planning, we adopt language-based metrics to evaluate the overall quality of the responses.

**Implementation Details.** We conduct experiments on one NVIDIA A40 GPU (48 GB memory), and train our framework for  $11k$  iterations with a batch size of 2 and a total training time of around 9 hours. We employ the AdamW [33] optimizer with an initial learning rate of  $2e^{-5}$ , a weight decay of 0.02, and a cosine scheduler with  $1.1k$  warm-up iterations. We adopt LLaMA-3-8B-Instruct [1] as our multimodal LLM backbone and apply LoRA [19] with a rank of 16 for efficient fine-tuning. The weight  $w_l$  used in the proposed Dynamic Graph Modulation is set as 2.0.

### 5.2 Benchmarking with Existing Methods

Table 2 presents quantitative experiments on the ReasonPlan3D validation set, where all compared methods are trained and evaluated on the same ReasonPlan3D benchmark for fairness. We can observe that the proposed SHARP achieves superior performance across all evaluation metrics, demonstrating its superiority in activity reasoning, task planning, and inter-step route planning. The superior performance is largely attributed to two key factors. First, the proposed Progressive Plan Generation enforces the model to maintain contextual consistency throughout the plan generation process by referring to the plans generated in previous steps. Second, the proposed Dynamic Graph

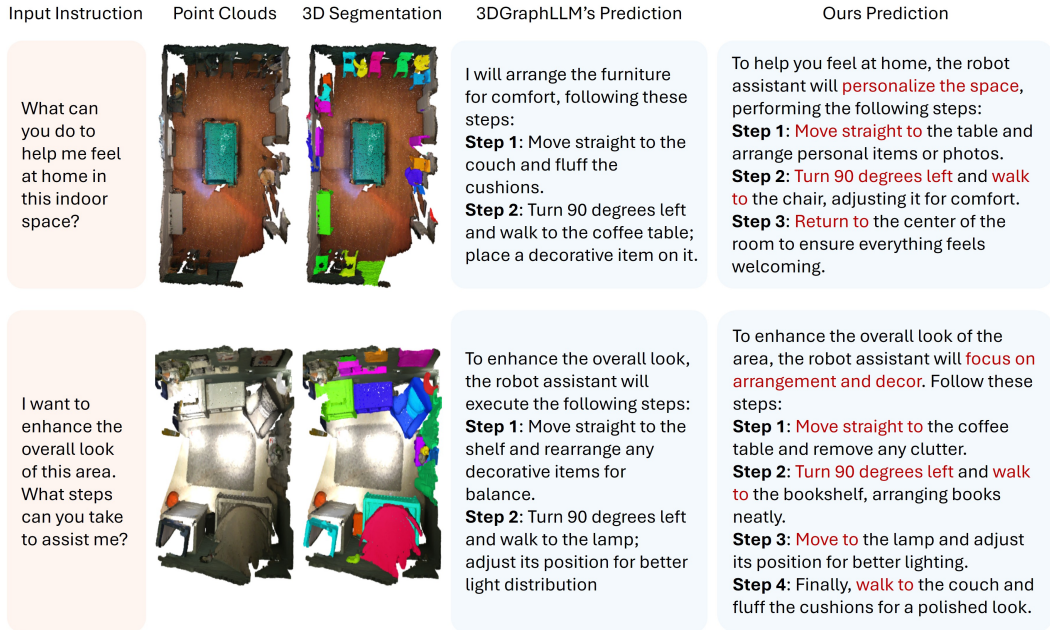


Figure 5: Activity reasoning and planning visualization over the ReasonPlan3D val set. Each example shows an implicit human instruction, the input point clouds of the 3D scene, the 3D segmentation of the scene, and the predictions from 3DGraphLLM and SHARP. Best viewed in color and zoom-in.

Table 3: Benchmarking on the ReasonPlan3D validation set for measuring activity reasoning performance with evaluation metrics BLEU-4, CIDEr, and METEOR. Best in **bold**, second underlined.

| Method          | BLEU-4       | CIDEr         | METEOR       |
|-----------------|--------------|---------------|--------------|
| 3D-LLM [18]     | 38.02        | 285.46        | 30.13        |
| LL3DA [5]       | 42.59        | 302.47        | 33.20        |
| Chat-Scene [20] | 45.26        | 313.90        | 34.42        |
| 3DGraphLLM [56] | 47.65        | <u>329.59</u> | <u>36.87</u> |
| SHARP (Ours)    | <b>50.28</b> | <b>359.53</b> | <b>38.35</b> |

Modulation guides the model toward critical objects and their spatial relations, enhancing 3D scene understanding and boosting route planning accuracy.

In addition, Table 3 presents the activity reasoning performance of SHARP and several state-of-the-art methods over the validation set of ReasonPlan3D. Our approach achieves superior performance across all metrics. Specifically, 3D-LLM [18], LL3DA [5], and Chat-Scene [20] do not employ a scene graph to explicitly guide the model’s awareness of critical objects, leading to suboptimal performance when dealing with the activity reasoning task where comprehending object relations plays an essential role. 3DGraphLLM [56] employs only scene graphs without scene-level embeddings of the global picture, leading to inferior 3D scene understanding and weaker performance for activity reasoning.

**Qualitative Benchmarking.** Figure 5 provides qualitative results on the validation set of ReasonPlan3D. Each example presents an implicit human instruction, an input point cloud, the corresponding 3D scene segmentation, and the generated textual answers by 3DGraphLLM [56] and the proposed SHARP. We can observe that SHARP can reason activities from the implicit input instructions accurately. Moreover, SHARP performs well in generating high-quality route plans as well. In both examples, SHARP surpasses 3DGraphLLM by generating more detailed steps, demonstrating its superior capability in complex planning tasks. Moreover, 3DGraphLLM introduces objects that do not exist in the scene, such as “couch”, “cushions”, and “coffee table” in the first example, while SHARP exhibits a more precise understanding of the 3D environment, generating plans that accurately reflect the objects present in the scene.

Table 4: Ablation studies over SHARP designs. PPG denotes Progressive Plan Generation, while DGM denotes Dynamic Graph Modulation. The symbol \* indicates the baseline. The best results are in **bold**.

| Index | PPG | DGM | BLEU-1       | BLEU-2       | BLEU-3       | BLEU-4       | CIDEr        | METEOR       | ROUGE        |
|-------|-----|-----|--------------|--------------|--------------|--------------|--------------|--------------|--------------|
| 1*    |     |     | 39.61        | 30.54        | 24.36        | 19.87        | 12.25        | 21.90        | 42.03        |
| 2     | ✓   |     | 51.46        | 38.49        | 29.35        | 23.82        | 23.80        | 27.09        | 43.39        |
| 3     | ✓   | ✓   | <b>52.22</b> | <b>39.30</b> | <b>30.58</b> | <b>24.59</b> | <b>25.51</b> | <b>27.51</b> | <b>43.76</b> |

Table 5: Ablation studies on the weight  $w_l$  as used in the proposed Dynamic Graph Modulation. The best results are in **bold**.

| Index | $w_l$ | BLEU-1       | BLEU-2       | BLEU-3       | BLEU-4       | CIDEr        | METEOR       | ROUGE        |
|-------|-------|--------------|--------------|--------------|--------------|--------------|--------------|--------------|
| 1     | 1.0   | 51.46        | 38.49        | 29.35        | 23.82        | 23.80        | 27.09        | 43.39        |
| 2     | 1.5   | 51.87        | 38.84        | 30.11        | 24.18        | 24.75        | 27.36        | 43.52        |
| 3     | 2.0   | <b>52.22</b> | <b>39.30</b> | <b>30.58</b> | <b>24.59</b> | <b>25.51</b> | <b>27.51</b> | <b>43.76</b> |
| 4     | 3.0   | 51.96        | 39.01        | 30.16        | 24.20        | 25.09        | 27.38        | 43.59        |

### 5.3 Ablation Study

We conduct ablation studies over the validation set of ReasonPlan3D to evaluate the effectiveness of our designs, including Progressive Plan Generation and Dynamic Graph Modulation as presented in the SHARP framework. In addition, we examine the effect of the weight  $w_l$  as used in the Dynamic Graph Modulation.

**Technical Designs.** We examine the effectiveness of two key designs in SHARP, namely, Progressive Plan Generation (PPG) and Dynamic Graph Modulation (DGM). As Table 4 shows, the baseline (in Row 1) without the two designs does not perform well across all evaluation metrics, largely because it struggles to maintain contextual consistency across steps and fails to capture the objects critical to the reasoned activity. Including the Progressive Plan Generation improves the performance clearly, as the step-by-step plan generation can refer to historical steps and thus preserve contextual information throughout the process. Finally, the best performance is obtained when both designs are included, largely because dynamically highlighting critical objects helps maintain the contextual consistency and allows SHARP to effectively capture implicit intentions and produce coherent and accurate step-by-step route plans.

**Effectiveness of  $w_l$ .** As defined in Equation 1, the weight  $w_l$  in the Dynamic Graph Modulation is introduced to highlight critical objects and their spatial relations relevant to the reasoned activity. We examine the effectiveness of  $w_l$  in Table 5. It can be observed that critical objects and their spatial relations are not well captured when  $w_l$  is set as 1.0, leading to degraded performance. Increasing  $w_l$  to 1.5 consistently improves performance, suggesting that placing greater emphasis on critical objects and their spatial relations can boost the model’s ability. Further increasing  $w_l$  to 2.0 achieves the best performance, confirming that guiding the model toward these crucial cues enhances the model’s planning ability. However, increasing  $w_l$  to 3.0 overemphasizes these objects and their spatial relations, leading to an imbalance among objects in the 3D scene that degrades the performance.

## 6 Conclusion

This paper presents a novel 3D Activity Reasoning and Planning task that reasons activities from implicit human intentions to satisfy their requirements, decomposes tasks into sequential steps, and plans inter-step routes in complex 3D environments. To this end, we introduce ReasonPlan3D, a large-scale benchmark containing diverse implicit user instructions, step-by-step task planning, inter-step route planning, and fine-grained segmentation annotations. On top of this, we propose a novel framework with a progressive plan generation mechanism to ensure that the generated steps remain contextually consistent. Moreover, a scene graph for capturing object relations is constructed, which is dynamically updated to emphasize critical objects and spatial relations for improving route planning accuracy. Extensive experiments confirm the effectiveness of our approach. Future work will investigate more challenging 3D scenarios, further expanding the potential of 3D scene understanding and human-robot interaction in real-world applications.

## References

- [1] AI@Meta. Llama 3 model card. 2024.
- [2] Daichi Azuma, Taiki Miyanishi, Shuhei Kurita, and Motoaki Kawanabe. Scanqa: 3d question answering for spatial scene understanding. In *Proceedings of the IEEE/CVF Conference on Computer Vision and Pattern Recognition*, pages 19129–19139, 2022.
- [3] Satyanjeev Banerjee and Alon Lavie. Meteor: An automatic metric for mt evaluation with improved correlation with human judgments. In *Proceedings of the acl workshop on intrinsic and extrinsic evaluation measures for machine translation and/or summarization*, pages 65–72, 2005.
- [4] Anthony Brohan, Yevgen Chebotar, Chelsea Finn, Karol Hausman, Alexander Herzog, Daniel Ho, Julian Ibarz, Alex Irpan, Eric Jang, Ryan Julian, et al. Do as i can, not as i say: Grounding language in robotic affordances. In *Conference on Robot Learning*, pages 287–318. PMLR, 2023.
- [5] Sijin Chen, Xin Chen, Chi Zhang, Mingsheng Li, Gang Yu, Hao Fei, Hongyuan Zhu, Jiayuan Fan, and Tao Chen. Ll3da: Visual interactive instruction tuning for omni-3d understanding reasoning and planning. In *Proceedings of the IEEE/CVF Conference on Computer Vision and Pattern Recognition*, pages 26428–26438, 2024.
- [6] Sijin Chen, Hongyuan Zhu, Xin Chen, Yinjie Lei, Gang Yu, and Tao Chen. End-to-end 3d dense captioning with vote2cap-detr. In *Proceedings of the IEEE/CVF Conference on Computer Vision and Pattern Recognition*, pages 11124–11133, 2023.
- [7] Yilun Chen, Shuai Yang, Haifeng Huang, Tai Wang, Ruiyuan Lyu, Runsen Xu, Dahua Lin, and Jiangmiao Pang. Grounded 3d-llm with referent tokens. *arXiv preprint arXiv:2405.10370*, 2024.
- [8] Zhenyu Chen, Ronghang Hu, Xinlei Chen, Matthias Nießner, and Angel X Chang. Unit3d: A unified transformer for 3d dense captioning and visual grounding. In *Proceedings of the IEEE/CVF International Conference on Computer Vision*, pages 18109–18119, 2023.
- [9] Angela Dai, Angel X Chang, Manolis Savva, Maciej Halber, Thomas Funkhouser, and Matthias Nießner. Scannet: Richly-annotated 3d reconstructions of indoor scenes. In *Proceedings of the IEEE/CVF Conference on Computer Vision and Pattern Recognition*, pages 5828–5839, 2017.
- [10] Jiajun Deng, Tianyu He, Li Jiang, Tianyu Wang, Feras Dayoub, and Ian Reid. 3d-llava: Towards generalist 3d llms with omni superpoint transformer. *arXiv preprint arXiv:2501.01163*, 2025.
- [11] Rao Fu, Jingyu Liu, Xilun Chen, Yixin Nie, and Wenhan Xiong. Scene-llm: Extending language model for 3d visual understanding and reasoning. *arXiv preprint arXiv:2403.11401*, 2024.
- [12] Lin Guan, Karthik Valmeekam, Sarath Sreedharan, and Subbarao Kambhampati. Leveraging pre-trained large language models to construct and utilize world models for model-based task planning. *Advances in Neural Information Processing Systems*, 36:79081–79094, 2023.
- [13] Ziyu Guo, Renrui Zhang, Xiangyang Zhu, Yiwen Tang, Xianzheng Ma, Jiaming Han, Kexin Chen, Peng Gao, Xianzhi Li, Hongsheng Li, et al. Point-bind & point-llm: Aligning point cloud with multi-modality for 3d understanding, generation, and instruction following. *arXiv preprint arXiv:2309.00615*, 2023.
- [14] Zoey Guo, Yiwen Tang, Ray Zhang, Dong Wang, Zhigang Wang, Bin Zhao, and Xuelong Li. Viewrefer: Grasp the multi-view knowledge for 3d visual grounding. In *Proceedings of the IEEE/CVF International Conference on Computer Vision*, pages 15372–15383, 2023.
- [15] Shibo Hao, Yi Gu, Haodi Ma, Joshua Jiahua Hong, Zhen Wang, Daisy Zhe Wang, and Zhiting Hu. Reasoning with language model is planning with world model. *Conference on Empirical Methods in Natural Language Processing*, 2023.
- [16] Rishi Hazra, Pedro Zuidberg Dos Martires, and Luc De Raedt. Saycanpay: Heuristic planning with large language models using learnable domain knowledge. In *Proceedings of the AAAI Conference on Artificial Intelligence*, volume 38, pages 20123–20133, 2024.
- [17] Shuting He, Henghui Ding, Xudong Jiang, and Bihan Wen. Segpoint: Segment any point cloud via large language model. In *Proceedings of the IEEE/CVF European Conference on Computer Vision*, pages 349–367. Springer, 2024.
- [18] Yining Hong, Haoyu Zhen, Peihao Chen, Shuhong Zheng, Yilun Du, Zhenfang Chen, and Chuang Gan. 3d-llm: Injecting the 3d world into large language models. *Advances in Neural Information Processing Systems*, 36:20482–20494, 2023.

- [19] Edward J Hu, Yelong Shen, Phillip Wallis, Zeyuan Allen-Zhu, Yuanzhi Li, Shean Wang, Lu Wang, and Weizhu Chen. Lora: Low-rank adaptation of large language models. *arXiv preprint arXiv:2106.09685*, 2021.
- [20] Haifeng Huang, Yilun Chen, Zehan Wang, Rongjie Huang, Runsen Xu, Tai Wang, Luping Liu, Xize Cheng, Yang Zhao, Jiangmiao Pang, et al. Chat-scene: Bridging 3d scene and large language models with object identifiers. In *Advances in Neural Information Processing Systems*, 2024.
- [21] Haifeng Huang, Zehan Wang, Rongjie Huang, Luping Liu, Xize Cheng, Yang Zhao, Tao Jin, and Zhou Zhao. Chat-3d v2: Bridging 3d scene and large language models with object identifiers. *arXiv preprint arXiv:2312.08168*, 2023.
- [22] Jiangyong Huang, Silong Yong, Xiaojian Ma, Xiongkun Linghu, Puhao Li, Yan Wang, Qing Li, Song-Chun Zhu, Baoxiong Jia, and Siyuan Huang. An embodied generalist agent in 3d world. *arXiv preprint arXiv:2311.12871*, 2023.
- [23] Kuan-Chih Huang, Xiangtai Li, Lu Qi, Shuicheng Yan, and Ming-Hsuan Yang. Reason3d: Searching and reasoning 3d segmentation via large language model. *arXiv preprint arXiv:2405.17427*, 2024.
- [24] Pin-Hao Huang, Han-Hung Lee, Hwann-Tzong Chen, and Tyng-Luh Liu. Text-guided graph neural networks for referring 3d instance segmentation. In *Proceedings of the AAAI Conference on Artificial Intelligence*, volume 35, pages 1610–1618, 2021.
- [25] Shijia Huang, Yilun Chen, Jiaya Jia, and Liwei Wang. Multi-view transformer for 3d visual grounding. In *Proceedings of the IEEE/CVF Conference on Computer Vision and Pattern Recognition*, pages 15524–15533, 2022.
- [26] Wenlong Huang, Pieter Abbeel, Deepak Pathak, and Igor Mordatch. Language models as zero-shot planners: Extracting actionable knowledge for embodied agents. In *International Conference on Machine Learning*, pages 9118–9147. PMLR, 2022.
- [27] Wenlong Huang, Fei Xia, Ted Xiao, Harris Chan, Jacky Liang, Pete Florence, Andy Zeng, Jonathan Tompson, Igor Mordatch, Yevgen Chebotar, et al. Inner monologue: Embodied reasoning through planning with language models. *Conference on Robot Learning*, 2023.
- [28] Xueying Jiang, Lewei Lu, Ling Shao, and Shijian Lu. Multimodal 3d reasoning segmentation with complex scenes. *arXiv preprint arXiv:2411.13927*, 2024.
- [29] Weitai Kang, Mengxue Qu, Jyoti Kini, Yunchao Wei, Mubarak Shah, and Yan Yan. Intent3d: 3d object detection in rgb-d scans based on human intention. *arXiv preprint arXiv:2405.18295*, 2024.
- [30] Boyi Li, Philipp Wu, Pieter Abbeel, and Jitendra Malik. Interactive task planning with language models. *Transactions on Machine Learning Research*, 2025.
- [31] Chengshu Li, Ruohan Zhang, Josiah Wong, Cem Gokmen, Sanjana Srivastava, Roberto Martín-Martín, Chen Wang, Gabrael Levine, Wensi Ai, Benjamin Martinez, et al. Behavior-1k: A human-centered, embodied ai benchmark with 1,000 everyday activities and realistic simulation. *Conference on Robot Learning*, 2022.
- [32] Chin-Yew Lin. Rouge: A package for automatic evaluation of summaries. In *Text summarization branches out*, pages 74–81, 2004.
- [33] Ilya Loshchilov and Frank Hutter. Decoupled weight decay regularization. *International Conference on Learning Representations*, 2019.
- [34] Xiaojian Ma, Silong Yong, Zilong Zheng, Qing Li, Yitao Liang, Song-Chun Zhu, and Siyuan Huang. Sqa3d: Situated question answering in 3d scenes. *International Conference on Learning Representations*, 2023.
- [35] Yunze Man, Liang-Yan Gui, and Yu-Xiong Wang. Situational awareness matters in 3d vision language reasoning. In *Proceedings of the IEEE/CVF Conference on Computer Vision and Pattern Recognition*, pages 13678–13688, 2024.
- [36] Kolby Nottingham, Prithviraj Ammanabrolu, Alane Suhr, Yejin Choi, Hannaneh Hajishirzi, Sameer Singh, and Roy Fox. Do embodied agents dream of pixelated sheep: Embodied decision making using language guided world modelling. In *International Conference on Machine Learning*, pages 26311–26325. PMLR, 2023.

- [37] Kishore Papineni, Salim Roukos, Todd Ward, and Wei-Jing Zhu. Bleu: a method for automatic evaluation of machine translation. In *Proceedings of the 40th annual meeting of the Association for Computational Linguistics*, pages 311–318, 2002.
- [38] Maria Parilli, Alexandros Delitzas, Nikolas Hars, Georgios Vlassis, Sotirios Anagnostidis, Gregor Bachmann, and Thomas Hofmann. Clip-guided vision-language pre-training for question answering in 3d scenes. In *Proceedings of the IEEE/CVF Conference on Computer Vision and Pattern Recognition*, pages 5607–5612, 2023.
- [39] Zhipeng Qian, Yiwei Ma, Jiayi Ji, and Xiaoshuai Sun. X-refseg3d: Enhancing referring 3d instance segmentation via structured cross-modal graph neural networks. In *Proceedings of the AAAI Conference on Artificial Intelligence*, volume 38, pages 4551–4559, 2024.
- [40] Abhinav Rajvanshi, Karan Sikka, Xiao Lin, Bhoram Lee, Han-Pang Chiu, and Alvaro Velasquez. Saynav: Grounding large language models for dynamic planning to navigation in new environments. In *Proceedings of the AAAI Conference on Artificial Intelligence*, volume 34, pages 464–474, 2024.
- [41] Krishan Rana, Jesse Haviland, Sourav Garg, Jad Abou-Chakra, Ian Reid, and Niko Suenderhauf. Sayplan: Grounding large language models using 3d scene graphs for scalable robot task planning. In *Conference on Robot Learning*, pages 23–72. PMLR, 2023.
- [42] David Rozenberszki, Or Litany, and Angela Dai. Language-grounded indoor 3d semantic segmentation in the wild. In *Proceedings of the IEEE/CVF European Conference on Computer Vision*, pages 125–141. Springer, 2022.
- [43] Manolis Savva, Abhishek Kadian, Oleksandr Maksymets, Yili Zhao, Erik Wijmans, Bhavana Jain, Julian Straub, Jia Liu, Vladlen Koltun, Jitendra Malik, et al. Habitat: A platform for embodied ai research. In *Proceedings of the IEEE/CVF International Conference on Computer Vision*, pages 9339–9347, 2019.
- [44] Mohit Shridhar, Jesse Thomason, Daniel Gordon, Yonatan Bisk, Winson Han, Roozbeh Mottaghi, Luke Zettlemoyer, and Dieter Fox. Alfred: A benchmark for interpreting grounded instructions for everyday tasks. In *Proceedings of the IEEE/CVF Conference on Computer Vision and Pattern Recognition*, pages 10740–10749, 2020.
- [45] Ishika Singh, Valts Blukis, Arsalan Mousavian, Ankit Goyal, Danfei Xu, Jonathan Tremblay, Dieter Fox, Jesse Thomason, and Animesh Garg. Progprompt: Generating situated robot task plans using large language models. In *International Conference on Robotics and Automation*, pages 11523–11530. IEEE, 2023.
- [46] Chan Hee Song, Jiaman Wu, Clayton Washington, Brian M Sadler, Wei-Lun Chao, and Yu Su. Llm-planner: Few-shot grounded planning for embodied agents with large language models. In *Proceedings of the IEEE/CVF International Conference on Computer Vision*, pages 2998–3009, 2023.
- [47] Haotian Sun, Yuchen Zhuang, Lingkai Kong, Bo Dai, and Chao Zhang. Adaplaner: Adaptive planning from feedback with language models. *Advances in Neural Information Processing Systems*, 36, 2024.
- [48] Hugo Touvron, Thibaut Lavril, Gautier Izacard, Xavier Martinet, Marie-Anne Lachaux, Timothée Lacroix, Baptiste Rozière, Naman Goyal, Eric Hambro, Faisal Azhar, et al. Llama: Open and efficient foundation language models. *arXiv preprint arXiv:2302.13971*, 2023.
- [49] Ramakrishna Vedantam, C Lawrence Zitnick, and Devi Parikh. Cider: Consensus-based image description evaluation. In *Proceedings of the IEEE/CVF Conference on Computer Vision and Pattern Recognition*, pages 4566–4575, 2015.
- [50] Zehan Wang, Haifeng Huang, Yang Zhao, Ziang Zhang, and Zhou Zhao. Chat-3d: Data-efficiently tuning large language model for universal dialogue of 3d scenes. *arXiv preprint arXiv:2308.08769*, 2023.
- [51] Changli Wu, Yiwei Ma, Qi Chen, Haowei Wang, Gen Luo, Jiayi Ji, and Xiaoshuai Sun. 3d-stmn: Dependency-driven superpoint-text matching network for end-to-end 3d referring expression segmentation. In *Proceedings of the AAAI Conference on Artificial Intelligence*, volume 38, pages 5940–5948, 2024.
- [52] Zhenyu Wu, Ziwei Wang, Xiuwei Xu, Jiwen Lu, and Haibin Yan. Embodied task planning with large language models. *arXiv preprint arXiv:2307.01848*, 2023.
- [53] Jianing Yang, Xuweiyi Chen, Shengyi Qian, Nikhil Madaan, Madhavan Iyengar, David F Fouhey, and Joyce Chai. Llm-grounder: Open-vocabulary 3d visual grounding with large language model as an agent. In *International Conference on Robotics and Automation*, pages 7694–7701. IEEE, 2024.

- [54] Jingkang Yang, Yuhao Dong, Shuai Liu, Bo Li, Ziyue Wang, Haoran Tan, Chencheng Jiang, Jiamu Kang, Yuanhan Zhang, Kaiyang Zhou, et al. Octopus: Embodied vision-language programmer from environmental feedback. In *Proceedings of the IEEE/CVF European Conference on Computer Vision*, pages 20–38. Springer, 2024.
- [55] Minjong Yoo, Jinwoo Jang, Wei-Jin Park, and Honguk Woo. Exploratory retrieval-augmented planning for continual embodied instruction following. *Advances in Neural Information Processing Systems*, 37:67034–67060, 2025.
- [56] Tatiana Zemsikova and Dmitry Yudin. 3dgraphllm: Combining semantic graphs and large language models for 3d scene understanding. *arXiv preprint arXiv:2412.18450*, 2024.
- [57] Zhuofan Zhang, Ziyu Zhu, Pengxiang Li, Tengyu Liu, Xiaojian Ma, Yixin Chen, Baoxiong Jia, Siyuan Huang, and Qing Li. Task-oriented sequential grounding and navigation in 3d scenes. *arXiv preprint arXiv:2408.04034*, 2024.
- [58] Ziyu Zhu, Xiaojian Ma, Yixin Chen, Zhidong Deng, Siyuan Huang, and Qing Li. 3d-vista: Pre-trained transformer for 3d vision and text alignment. In *Proceedings of the IEEE/CVF International Conference on Computer Vision*, pages 2911–2921, 2023.
- [59] Ziyu Zhu, Zhuofan Zhang, Xiaojian Ma, Xuesong Niu, Yixin Chen, Baoxiong Jia, Zhidong Deng, Siyuan Huang, and Qing Li. Unifying 3d vision-language understanding via promptable queries. In *Proceedings of the IEEE/CVF European Conference on Computer Vision*, pages 188–206. Springer, 2024.